

Supplementary Information

An anthracene-based Hydrogen-bonded Organic Framework as Bifunctional Fluorescent Sensor for the Detection of γ -Aminobutyric Acid and Nitrofurazone

Yanhong Liu,[†] Xin Xu, [†] and Bing Yan^{*,†}

[†]School of Chemical Science and Engineering, Tongji University, 1239 Siping Road,
Shanghai 200092, China

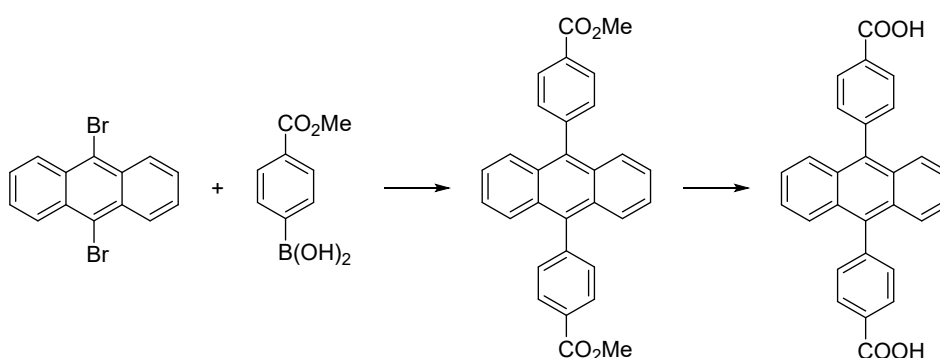
* Corresponding author: Bing Yan, Email: byan@tongji.edu.cn

Materials and instruments

The H₂DBA ligand was prepared according to the literature method¹. All reagents and solvents used in the whole experiments were commercially available and used without further purification. 2-fluorobenzoic acid (2-FBA), *N,N*-dimethylformamide (DMF), HNO₃, NaOH, HCl, Dimethyl-*d*₆ sulfoxide (DMSO-*d*₆), γ -aminobutyric acid (GABA), nitrofurazone (NFZ) and furazolidone (FZ) were purchased from Sigma-Aldrich Chemicals. The solid medicines of urea, L-proline, creatine, glucose, creatinine, Na₂SO₄, KCl, NaCl, NH₄Cl, MgCl₂, CaCl₂, streptomycin sulfate, sulfadiazine, gentamicin sulfate, flumequine, levofloxacin and metronidazole were procured from Aladdin Chemistry Co. (Shanghai, China). Goat serum and artificial urine was purchased from Shanghai Sangon Biotechnology Co., Ltd. (Shanghai, China). Deionized water was used throughout the experiments.

Single crystal X-ray diffraction data was collected on Bruker D8 Venture diffractometer at 150 K. NMR spectra were recorded on Bruker Avance III HD 600 MHz at ambient temperature. The residual peak of deuterated solvent was used as a reference for ¹H chemical shifts. The following abbreviations (or combinations thereof) were used to explain the multiplicities: s = singlet, d = doublet, t = triplet, q = quartet, m = multiplet, br = broad. Powder X-ray diffraction (PXRD) data were collected on a Bruker D8 Advance diffractometer with Cu K α radiation operating at 40 kV and 40 mA. All samples were ground and installed as powders onto a Si sample holder. PXRD patterns were recorded at $2\theta = 5\text{--}50^\circ$, with an exposure time of 0.1 s per step and a step size of 0.02° . Thermogravimetric analysis (TGA) was carried out on a Netzsch STA 449C system analyzer under air atmosphere at a heating rate of $15\text{ }^\circ\text{C min}^{-1}$ in the temperature range of $40\text{--}800\text{ }^\circ\text{C}$. The surface areas were calculated by the Brunauer–Emmett–Teller (BET) method. Fourier transform infrared (FTIR) spectroscopy were measured on a Nexus 912 AO446 infrared spectrum radiometer in the wavenumber range of $4000\text{--}400\text{ cm}^{-1}$ using KBr pellets. Element analysis were performed on a VARIO ELIII elemental instrument. The fluorescence spectra for the samples were obtained on an Edinburgh FLS920 spectrophotometer with a 450 W xenon lamp as the source of excitation employing an appropriate cutoff filter. The decays were recorded

using pulsed flash lamps. UV-vis absorption spectra were determined on an Agilent 8453 spectrometer. Commission Internationale de l'Eclairage (CIE) color coordinates were calculated based on the international CIE standards. Scanning electron microscopy (SEM) images were recorded on an S-4800 field emission scanning electron microscope (Hitachi, Tokyo, Japan).



A mixture of 9,10-dibromoanthracene (1.8 g, 5.4 mmol), 4-methoxycarbonylphenylboronic acid (2.92 g, 16.2 mmol), CsF (3 g, 19.7 mmol) and Pd(PPh₃)₄ (0.17 g, 0.15 mmol) was placed in a 150 mL two-necked shclenk flak and pumped for 15 min. 80 mL of degassed 1,2-dimethoxyethane was added through a canula. The mixture was heated to reflux under argon atmosphere for 60 h. After the mixture was cooled to room temperature, the solvent was removed. The yellow residue was suspended in water (40 mL) and extracted with CH₂Cl₂. After drying the mixed organic phase over MgSO₄ and removing the solvent, the crude product was purified by column chromatography (silica, CH₂Cl₂) to give the pure product of a yellow powder.

9,10-bis(p-(4-methoxycarbonyl)phenyl)anthracene (0.51 g, 1.15 mmol) was dissolved in 90 mL mixture of THF and MeOH (v/v = 2:1), 20 mL of a 20% KOH aqueous solution was added. The mixture was stirred to reflux for 12 h. The organic phase was removed under reduced pressure and the resulting suspension was diluted with 20 mL water. The precipitate formed by acidification with diluted hydrochloric acid was filtered and washed with water several times.

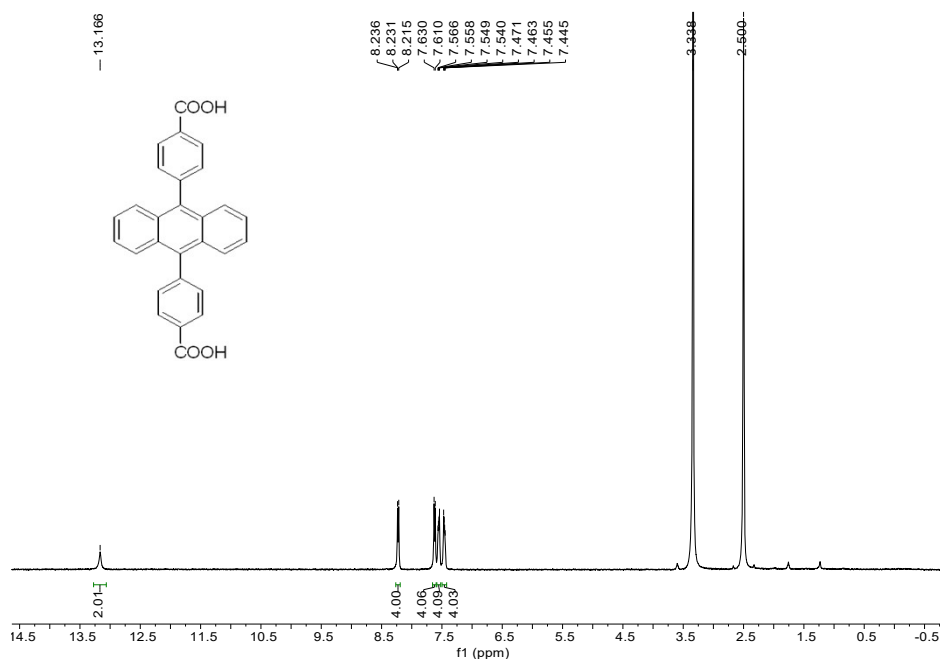


Fig. S1. ^1H NMR spectra of H_2DBA .

Table S1. Crystal data and refinement parameters for **HOF-DBA**.

Identification code	HOF-DBA
Chemical formula	$\text{C}_{17}\text{H}_{16}\text{NO}_3$
Formula weight	282.31
Crystal Colour	Bright yellow
Temperature (K)	150(2)
Crystal System	Triclinic
Space Group	<i>P</i> -1
<i>a</i> (Å)	7.2169
<i>b</i> (Å)	8.9309
<i>c</i> (Å)	12.2087
α (°)	70.598
β (°)	76.912
γ (°)	77.565
<i>Z</i>	2
<i>V</i> (Å ³)	714.47(7)
D_{calc} (g cm ⁻³)	1.312
<i>F</i> (000)	298.0
μ (mm ⁻¹)	0.090
<i>R</i> (int)	0.0437
Number of parameters	210
GOF on <i>F</i> ²	1.014
R_1^{a} [<i>I</i> > 2σ(<i>I</i>)]	0.0581
wR_2^{b} (all data)	0.1721
CCDC	2080731

$$R_1 = \frac{\sum(|F_o| - |F_c|)}{\sum|F_o|}; wR_2 = \left\{ \frac{\sum w(|F_o|^2 - |F_c|^2)^2}{\sum w|F_o|^2} \right\}^{1/2}.$$

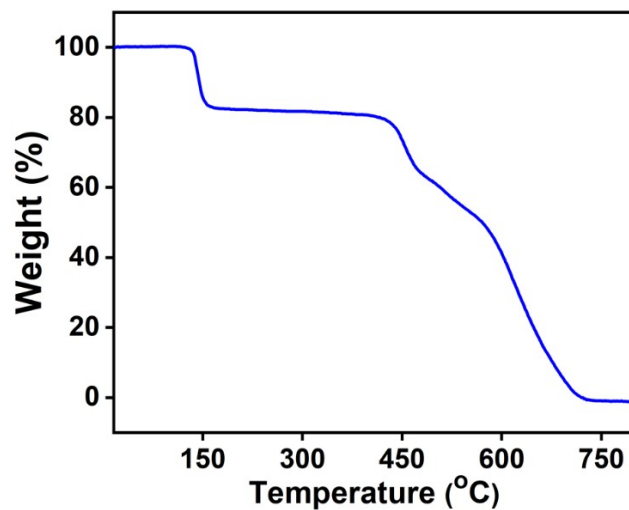


Fig. S2. TGA traces of HOF-DBA ranging from room temperature to 750 °C.

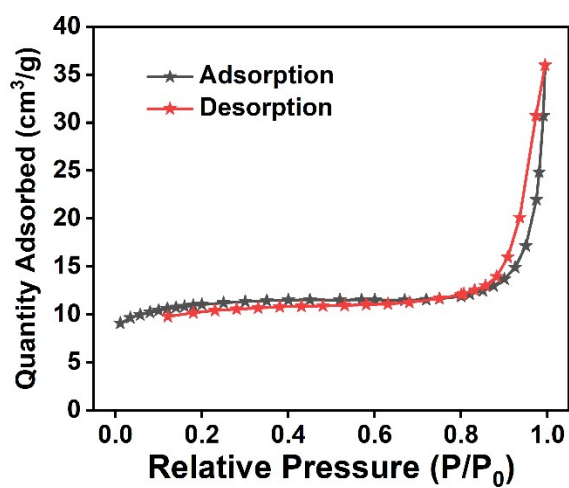


Fig. S3. N₂ sorption isotherms of HOF-DBA at 77 K.

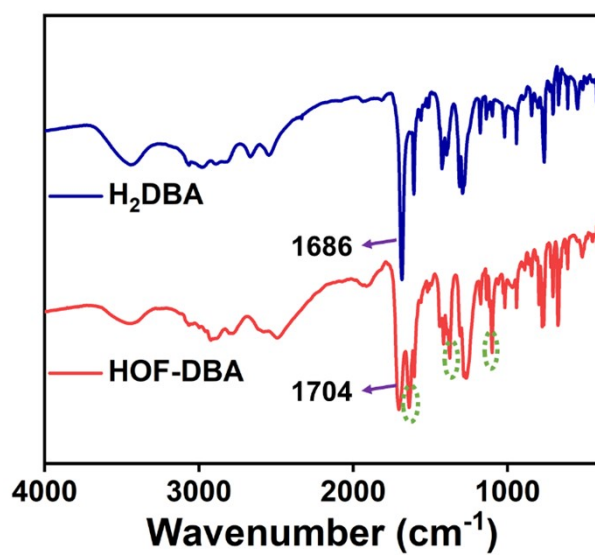


Fig. S4. FT-IR spectra of H₂DBA (blue), HOF-DBA (red).

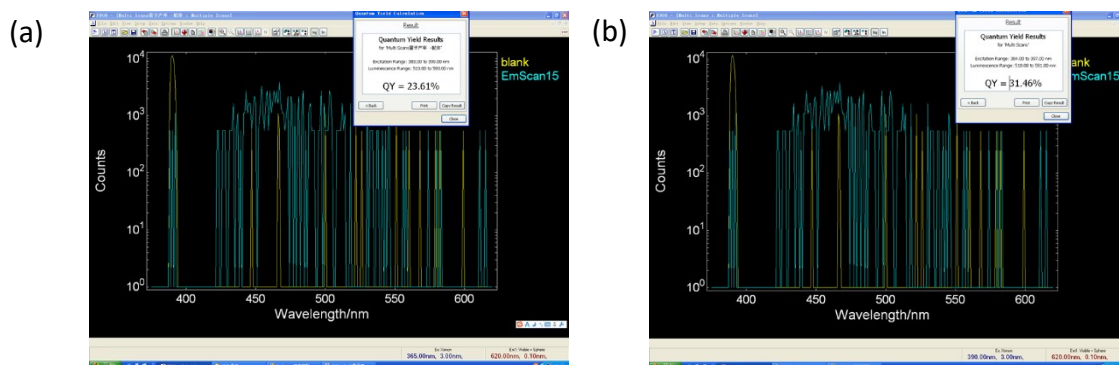


Fig. S5. (a) The luminescence quantum yield of H₂DBA and (b) HOF-DBA.

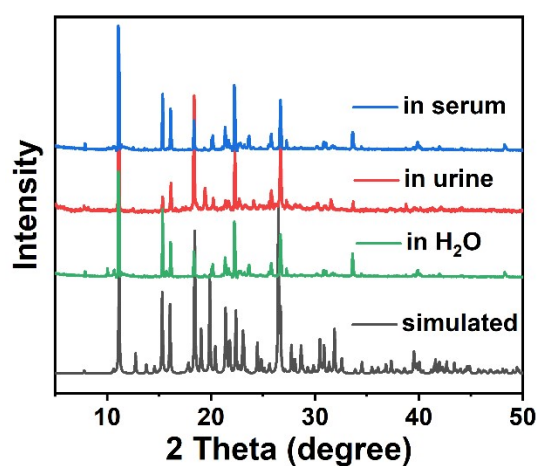


Fig. S6. Powder X-ray diffraction (PXRD) profiles for simulated HOF-DBA (black) and HOF-DBA samples soaked in aqueous solutions (green), in urine (red), and in serum (blue) for 24 h.

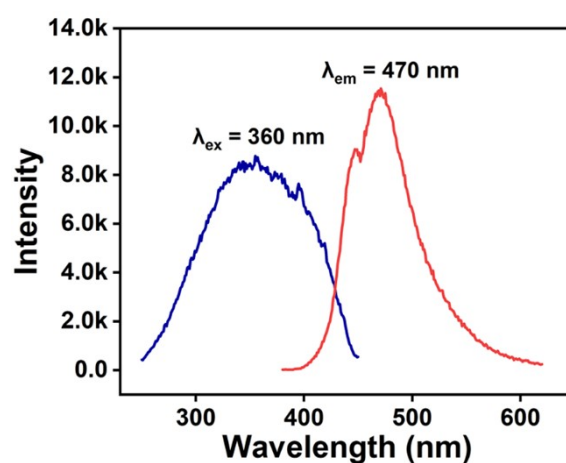


Fig. S7. The excitation and emission spectra of HOF-DBA in water solution.

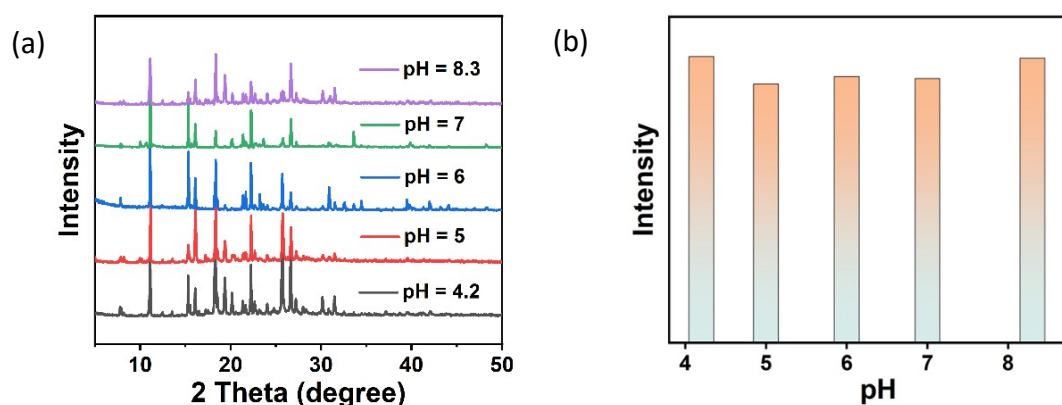


Fig. S8. (a) PXRD patterns and (b) the histogram of luminescence of HOF-DBA after immersion in pH = 4.2–8.3 solutions for 24 h.

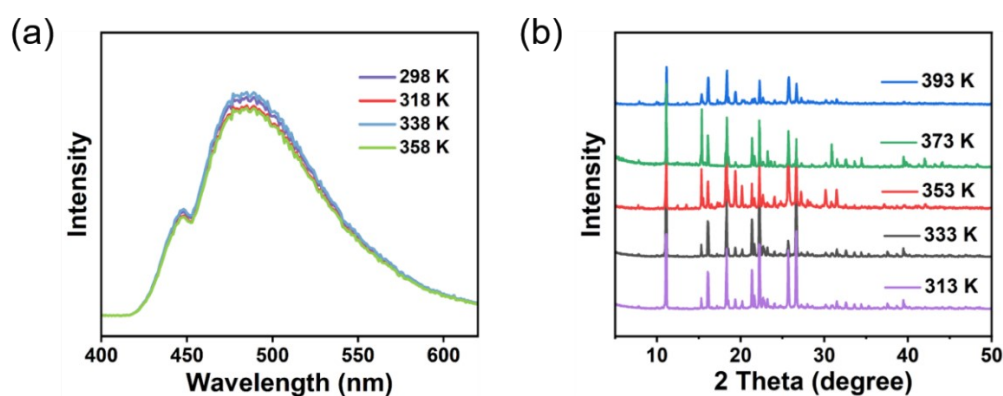


Fig. S9. (a) Dependence of emission intensity for HOF-DBA on temperature (298–358 K) upon $\lambda_{\text{ex}} = 360$ nm. (b) The variable-temperature PXRD patterns of HOF-DBA in the range of 313–393 K.

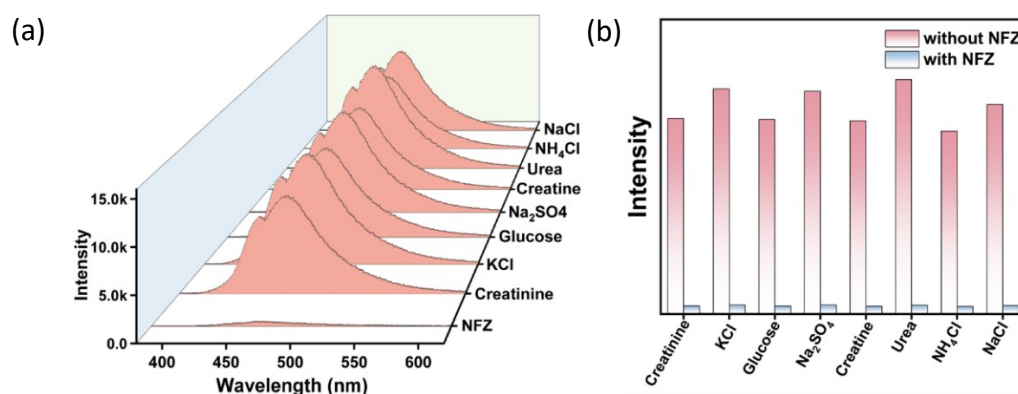


Fig. S10. (a) Emission spectra of HOF-DBA in NFZ and various components (10^{-3} M) in urine system. (b) Corresponding intensity at 470 nm for HOF-DBA toward various components in urine system.

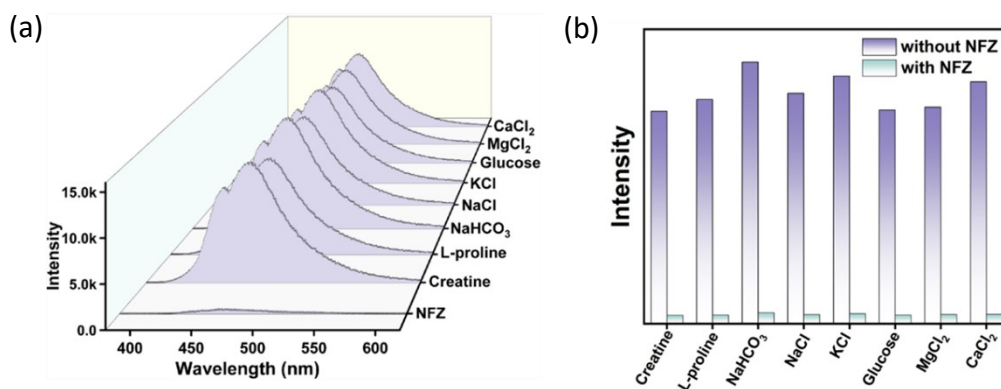


Fig. S11. (a) Emission spectra of HOF-DBA in NFZ and various components (10^{-3} M) in serum system. (b) Corresponding intensity at 470 nm for HOF-DBA toward various components in serum system.

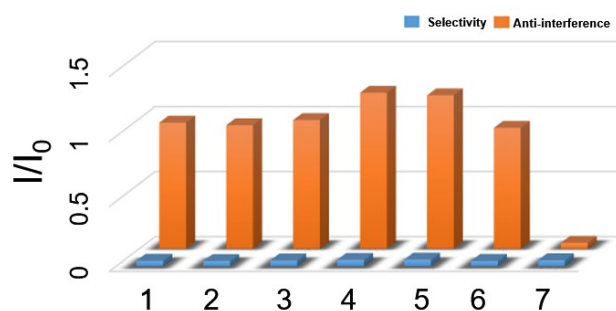


Fig. S12. Selectivity and anti-interference ability of HOF-DBA with NFZ in the presence and absence of different interfering compounds (1, streptomycin sulfate; 2, sulfadiazine; 3, gentamicin sulfate; 4, flumequine; 5, levofloxacin; 6, metronidazole; 7, NFZ). The concentrations of NFZ and interfering compounds are 10^{-3} M.

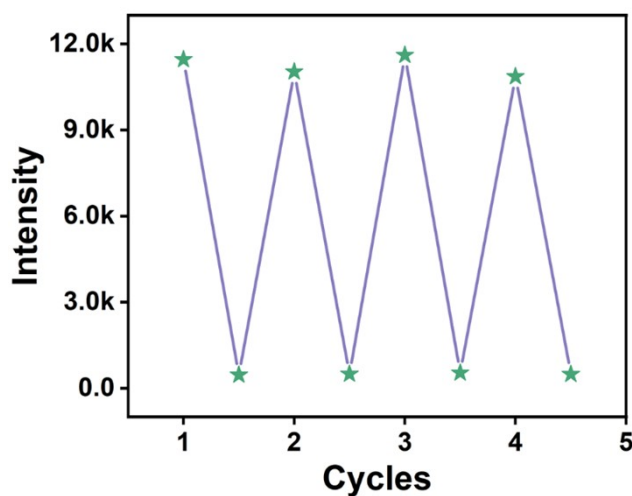


Fig. S13. The luminescence intensity of HOF-DBA toward NFZ after four recycles.

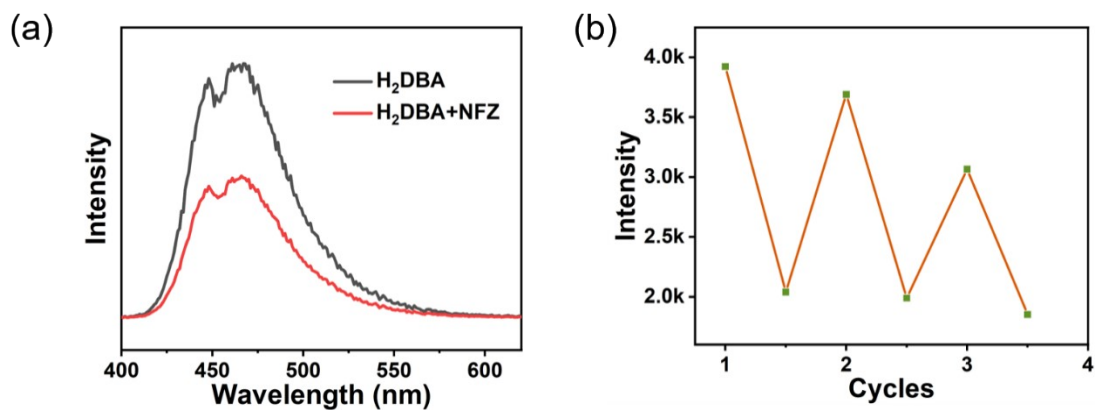


Fig. S14 (a) Emission spectrum of H₂DBA and H₂DBA + NFZ ($\lambda_{\text{ex}} = 360$ nm). (b) The luminescence intensity of H₂DBA toward NFZ after three recycles.

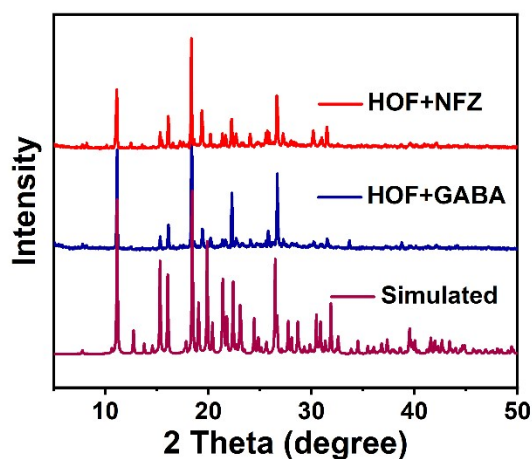


Fig. S15. PXRD patterns of HOF-DBA and after sensing GABA (blue) and NFZ (red).

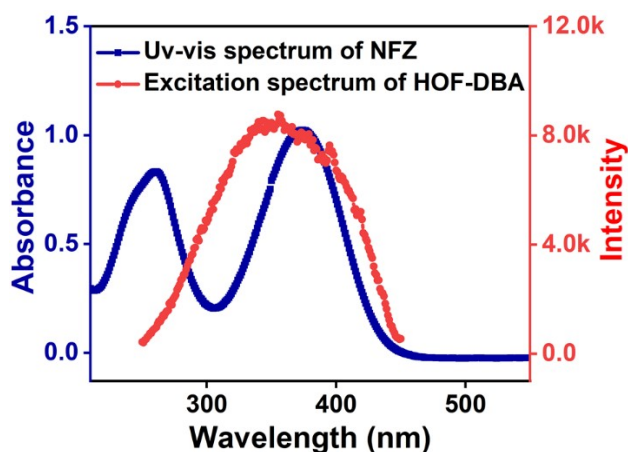


Fig. S16. The UV-vis spectrum of NFZ and excitation spectrum of HOF-DBA.

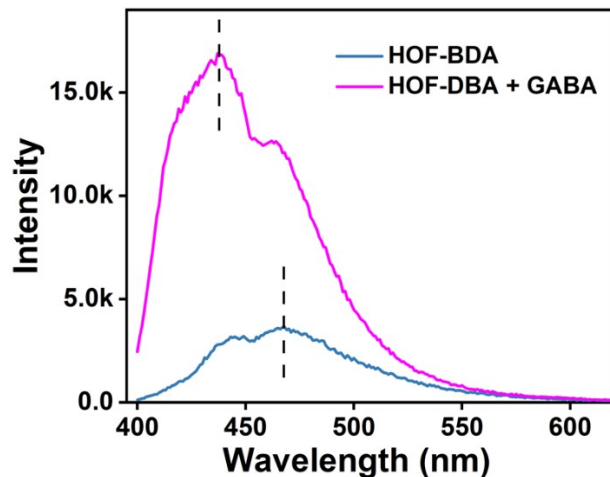


Fig. S17. Emission spectrum of HOF-DBA and HOF-DBA + GABA ($\lambda_{\text{ex}} = 360$ nm).

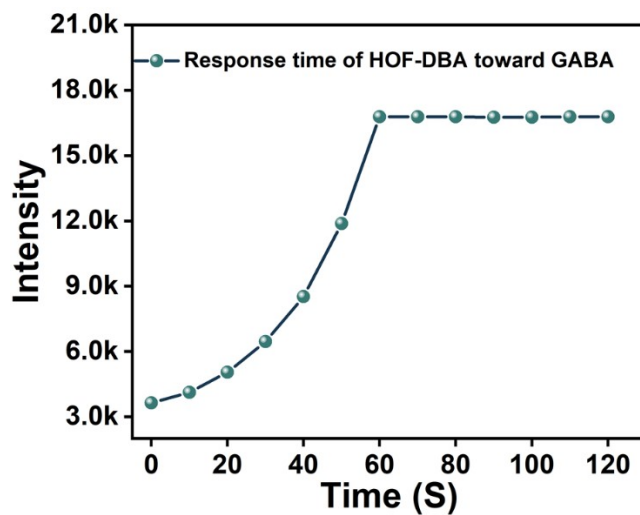


Fig. S18. Time-dependent luminescence intensity of HOF-DBA toward GABA.

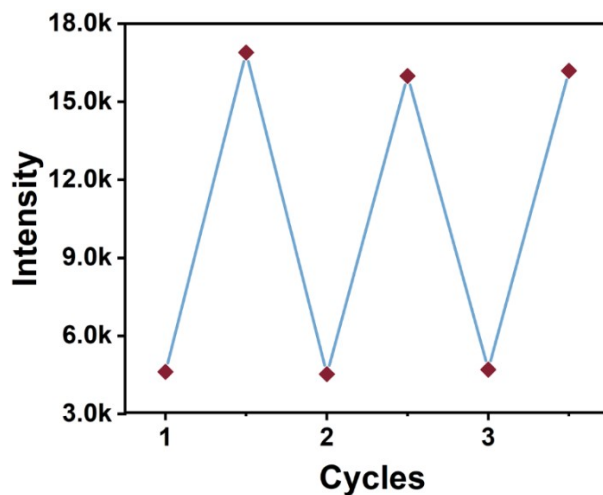


Fig. S19. The luminescence intensity of HOF-DBA toward GABA after three recycles.

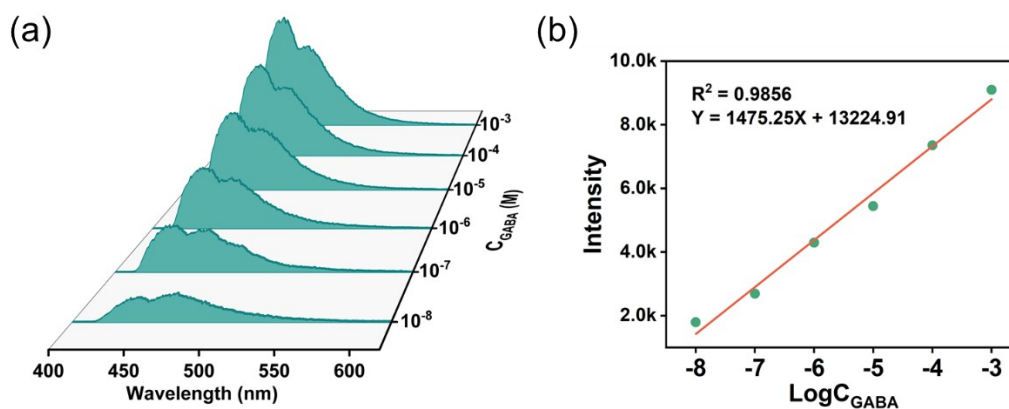


Fig. S20. (a) The emission spectrums ($\lambda_{\text{ex}} = 360$ nm) of HOF-DBA immersed in various concentration of GABA in serum (10^{-8} – 10^{-3} M); (b) Dependence of emission intensity of HOF-DBA on concentration of GABA in serum.

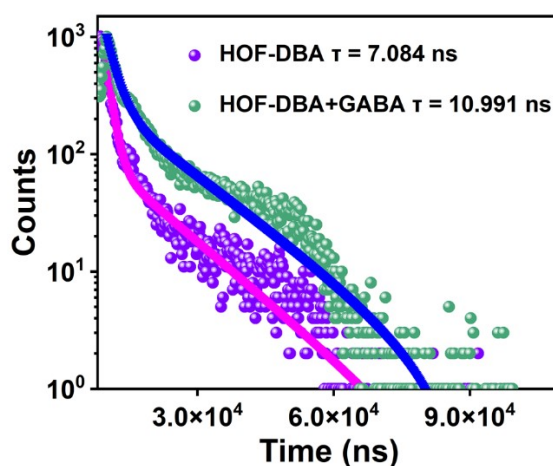


Fig. S21. Decay lifetimes of 470 nm emission peak for HOF-DBA and HOF-DBA+GABA ($C = 10^{-3}$ M) ($\lambda_{\text{ex}} = 360$ nm).

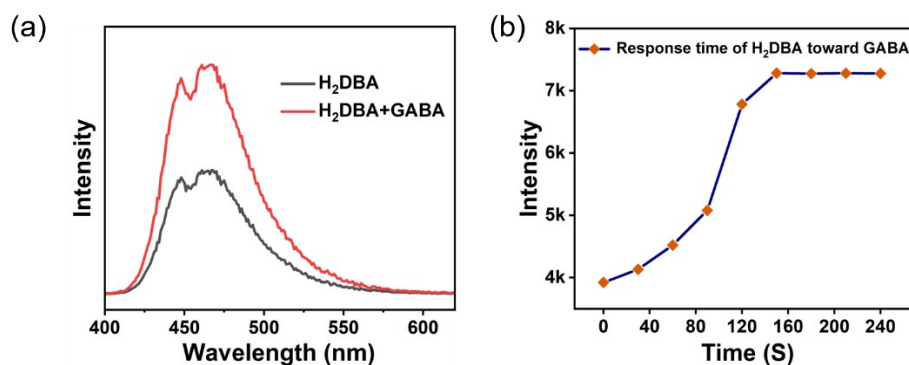


Fig. S22. (a) Emission spectrum of H₂DBA and H₂DBA + GABA ($\lambda_{\text{ex}} = 360$ nm). (b) Time-dependent luminescence intensity of H₂DBA toward GABA.

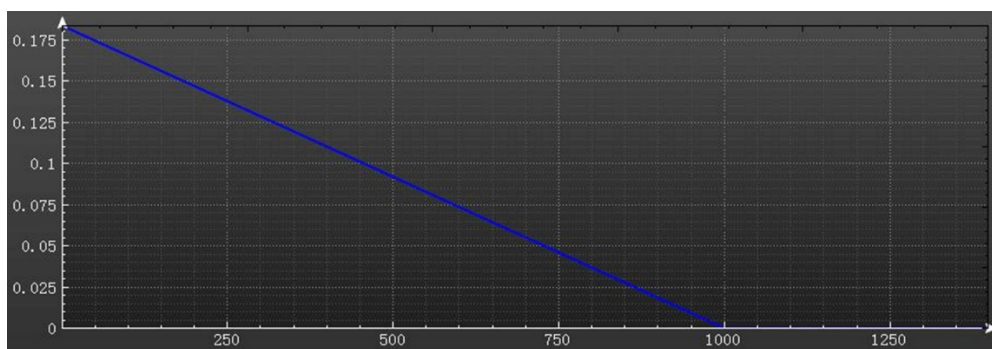


Fig. S23. Network training curve of the BPNN.

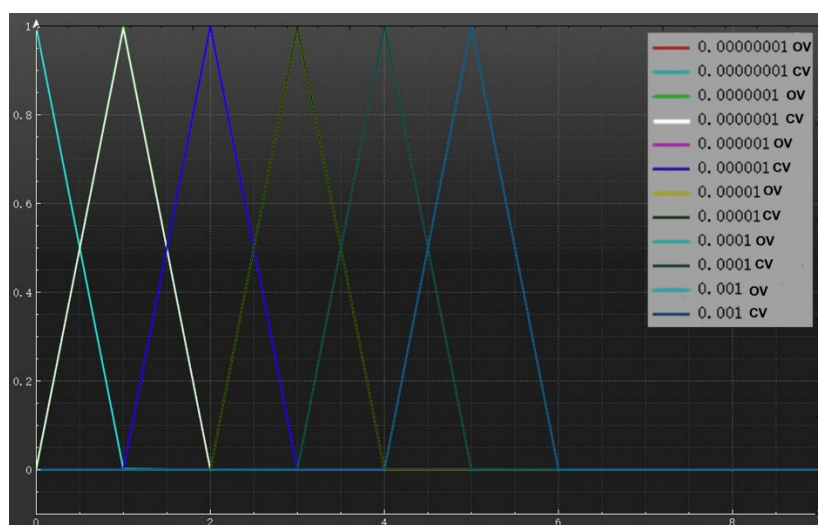


Fig. S24. Deviation curve of the BPNN (OV: original value; CV: calculated value).

In Fig. S24, there are two type of curves respectively representing original value (OV) and calculated value (CV). All curves of OV are overlapped well with the curves of CV, which indicating the low deviation between original and calculated values of output information. Therefore, all curves of OV can not be seen and all curves of CV can only be seen.

Table S2. Determination of NFZ in serum and urine samples.

Sample	NFZ added ($\mu\text{mol/L}$)	NFZ found ($\mu\text{mol/L}$)	Recovery (%)	R.S.D. (n = 3) (%)
serum	0.1	0.105	105	2.26
	5	4.859	97.18	3.48

	10	10.321	103.21	1.89
	0.1	0.097	97	2.18
urine	5	5.141	102.82	1.95
	10	10.483	104.83	4.12

Table S3. Summary of input and output information during the training of BPNN for GABA detection.

Input (I/I ₀)		Output [concentration of GABA (M)]					
1	0	10 ⁻⁸	10 ⁻⁷	10 ⁻⁶	10 ⁻⁵	10 ⁻⁴	10 ⁻³
1.27	1	0	0	0	0	0	0
1.77	0	1	0	0	0	0	0
2.42	0	0	1	0	0	0	0
3.29	0	0	0	1	0	0	0
3.75	0	0	0	0	1	0	0
4.65	0	0	0	0	0	1	0

In Table S3, all data is used to training the BPNN. The I/I₀ values as input information are inputted in the input column of the BPNN. Various “0” and “1” inputted into the output column of the BPNN, in which “0” represents the false GABA concentration, and “1” represents the correct GABA concentration. All data is used to train the BPNN.

Table S4. Network structure information.

Network structure information		
Input layer	1 neurons	1 Paranoid
Hidden layer 1	6 neurons	1 Paranoid
Output layer	6 neurons	
Network type	FANN_NETTYPE_LA YER	
Training function	FANN_TRAIN_RPRO P	
Error function	FANN_ERRORFUNC _LINEAR	
Termination function	FANN_STOPFUNC_ MSE	
Hidden layer excitation function	FANN_SIGMOID_SY MMETRIC	
Output layer excitation function	FANN_SIGMOID_SY MMETRIC	
Network weight value		

Arrangement	Wire number	Output point	Input point	Weight value (W)
1	0	0	2	1500
	1	1	2	-1500
	2	0	3	7.56632
	3	1	3	3.61438
	4	0	4	1.15556
	5	1	4	0.211716
	6	0	5	1500
	7	1	5	-1500
	8	0	6	77.3405
	9	1	6	-1478.82
	10	0	7	13.4271
2	11	1	7	-2.07653
	12	2	9	8.64385
	13	3	9	-74.3199
	14	4	9	65.4009
	15	5	9	8.73719
	16	6	9	1.80722
	17	7	9	12.0294
	18	8	9	-5.98806
	19	2	10	4.8676
	20	3	10	-36.629
	21	4	10	152.772
	22	5	10	2.6805
	23	6	10	4.05031
	24	7	10	-38.999
	25	8	10	-3.0016
	26	2	11	165.899
	27	3	11	816.461
	28	4	11	-1500
	29	5	11	397.019
	30	6	11	24.7201
	31	7	11	-91.958
	32	8	11	4.95673
	33	2	12	36.4066
	34	3	12	160.064
	35	4	12	14.2532
	36	5	12	19.8049
	37	6	12	76.8273
	38	7	12	-46.6738
	39	8	12	-11.3956
	40	2	13	9.20155
	41	3	13	88.2249
	42	4	13	-288.537

43	5	13	17.5397
44	6	13	-1.87741
45	7	13	91.261
46	8	13	-26.8035
47	2	14	1500
48	3	14	1265.96
49	4	14	1450
50	5	14	1500
51	6	14	1500
52	7	14	1282.41
53	8	14	1450

Input / output column coefficients for manual calculation

Listing	Minimum	Maximum
1	1.35936	5.50874
0.00000001	0	1
0.0000001	0	1
0.000001	0	1
0.00001	0	1
0.0001	0	1
0.001	0	1

Deviation statistics: mean variance

Listing	All rows	Calculation line	Test line
0.00000001	1.42813e-06	1.42813e-06	0
0.0000001	4.46436e-06	4.46436e-06	0
0.000001	0	0	0
0.00001	0	0	0
0.0001	0	0	0
0.001	0	0	0

Table S5. The summary of mean square error (MSE), original value (OV), calculated value (CV), variance (Var.)

Input item	0.00000001 (MSE=1.42813e-06)			0.0000001 (MSE=4.46436e-06)			0.000001 (MSE=0)		
	OV.	CV.	Var.	OV.	CV.	Var.	OV.	CV.	Var.
1.4309	1	0.99697 1	9.17484 e-06	0	0.00423 45	1.7931e -05	0	0	0
1.9988	0	0.00218	4.7524e -06	1	0.99494	2.56036 e-05	0	0	0
2.7308	0	0	0	0	0.00086 75	7.52556 e-07	1	1	0
3.7113	0	0	0	0	0	0	0	0	0
4.2187	0	0	0	0	0	0	0	0	0
5.2333	0	0	0	0	0.00059	3.56409	0	0	0

					7	e-07			
0	0	0.00029 75	8.85063 e-08	0	0	0	0	0	0
0	0	0.00029 75	8.85063 e-08	0	0	0	0	0	0
0	0	0.00029 75	8.85063 e-08	0	0	0	0	0	0
0	0	0.00029 75	8.85063 e-08	0	0	0	0	0	0
Input item	0.00001 (MSE=0)			0.0001 (MSE=0)			0.001 (MSE=0)		
1	OV.	CV.	Var.	OV.	CV.	Var.	OV.	CV.	Var.
1.4309	0	0	0	0	0	0	0	0	0
1.9988	0	0	0	0	0	0	0	0	0
2.7308	0	0	0	0	0	0	0	0	0
3.7113	1	1	0	0	0	0	0	0	0
4.2187	0	0	0	1	1	0	0	0	0
5.2333	0	0	0	0	0	0	1	1	0
0	0	0	0	0	0	0	0	0	0
0	0	0	0	0	0	0	0	0	0
0	0	0	0	0	0	0	0	0	0
0	0	0	0	0	0	0	0	0	0

In Table S5, all data is utilized to test the BPNN. The I/I_0 as input information are inputted in the input column of the BPNN. Through the BPNN calculation, various values (0-1) can be outputted, in which the values close to "0" represents the false GABA concentration, the values close to "1" represents the correct GABA concentration. By comparing the OV with CV, the variance can be obtained, which suggests that the BPNN has a good accuracy for detecting GABA concentration.

Table S6. The summary of input and output information in real batch calculation during the test of BPNN.

Input data	Output data						
	I/I_0	0.00000001	0.0000001	0.000001	0.00001	0.0001	0.001
1.4309	0.996971	0.0042345	0	0	0	0	0
1.9988	0.00218	0.99494	0	0	0	0	0
2.7308	0	0.0008675	1	0	0	0	0
3.7113	0	0	0	1	0	0	0
4.2187	0	0	0	0	1	0	0
5.2333	0	0.000597	0	0	0	1	1

In Table S6, all data is utilized to test the BPNN. The I/I_0 values of every color as input information are inputted in the input column of the BPNN. Through the BPNN calculation, various values (0-1) can be acquired, in which the values close to "0" represents the false GABA concentration, and the values close to 1 represents the

correct GABA concentration.